Augmented Invariance Control for Impedance-controlled Robots with Safety Margins

Christoph Jähne *, **Sandra Hirche** *

* *Both authors are with the Chair of Information-oriented Control (ITR), Technical University of Munich, 80333 Germany (e-mail: c.jaehne@tum.de, hirche@lsr.ei.tum.de).*

Abstract: Various robotic applications require enforcing constraints, to achieve task performance or to hinder the robot from causing danger. Especially in human-robot-interaction, collision avoidance and velocity limits are crucial for safety. A promising approach to enforce adherence to safety margins is invariance control. Considering the system dynamics, it corrects a nominal control based on a switching policy. To overcome the resulting lack of smoothness in terms of control inputs and states, a control scheme is developed that adds dynamics to the input and thereby augments the system. In previous work it is shown that the closed loop system is stable in combination with an exponentially stabilizing nominal control. However, this could not be shown for impedance controlled robots. Therefore, in this paper, an augmented invariance control for robotic applications is developed and proven to be uniformly asymptotically stable with an impedance-type nominal control. The proposed control law is validated in experiments on a KUKA LWR4+ in a collision avoidance scenario demonstrating stable behaviour with improved smoothness and chattering characteristics while enforcing the imposed hard constraints.

Keywords: invariance control, hard constraints, smoothness, continuous actuation, safety margins, robot, impedance control, asymptotic stability.

1. INTRODUCTION

Robots are gradually expanding their field of application from purely industrial settings to e.g. service robotics and enter domestic domains. This involves facing dynamic environments that are hard to predict or plan. Especially in human-robot interaction this raises the need for control features that ensure safety for both robot and human during operation. A safe solution is reactive collision avoidance that prevents unintended contacts between robot and environment. To achieve this, various methods exist. Model predictive control (MPC) (Mayne et al., 2000) and the command governor approach (Angeli and Mosca, 1999) are based on optimization and allow to consider hard constraints to states, inputs or outputs but may be computationally too expensive in real-time application. Virtual potential fields enable the derivation of repelling forces that are added to the control input of the robot (Rimon and Koditschek, 1992) but without considering a dynamic model of the system, adherence to constraints cannot be guaranteed though. Another alternative to enforce constraints is the inclusion of control barrier functions as in (Rauscher et al., 2016) that serve to impose constraints to a convex optimization problem for supervising a nominal control signal w.r.t. an arbitrary number of boundaries. However, barrier functions tend to infinity approaching the barriers and are therefore only defined inside the constraint admissible area. In real applications, minor boundary violations cannot be excluded due to sensor noise. A closely related approach is invariance control. It reactively supervises a nominal control scheme and corrects it whenever necessary in order to keep boundaries that are defined as hard constraints to the state space. Instead of barrier functions, invariance functions are derived from the system dynamics which are defined in the constraint admissible area as well as outside. This enables the system to recover from constraint violations. As shown in (Kimmel and Hirche, 2015) this also allows for dynamic boundaries which makes it appealing in human-robot-interaction. When facing dynamic sceneries, the set of considered boundaries needs to be updated online as a priori unknown or untracked objects/persons might enter the workspace of the robot. In addition limited capabilities of perception might not allow complete tracking of all obstacles at all time. Thus, jumps in the set of constraints cause abrupt and unforeseen reactions of the robot. In general, with the approach to invariance control described in (Kimmel and Hirche, 2015) and adapted from (Wolff and Buss, 2004), a smooth robot motion at the boundaries is hindered by switching between nominal and corrective control. This induces repeated jumps in the robots control input, especially when chattering occurs due to discrete implementation. On the long run, this potentially damages the actuation system and is highly undesired for smooth and intuitive human-robot interaction. In (Kimmel et al., 2016) we propose an approach to invariance control that allows to achieve smoothness requirements on states and control inputs by artificially augmenting the controlled system. Stability is proven, assuming an exponentially stable nominal control. However, most common control schemes for physical

human-robot-interaction such as impedance control could not be shown to be exponentially stable.
The contribution of this paper is the development of an augmented invariance control for impedance controlled robots. We show asymptotic stability for the augmented closed loop system. The functionality and stability of the approach are validated in experiments on a KUKA LWR4+. Chattering and smoothness characteristics in comparison with a non-augmented invariance control scheme indicate the advantages of the proposed control scheme.
The remainder of the this paper is organized as follows: Section 2 introduces system formulations and augmented invariance control. In Section 3, the theory is adapted to impedance-controlled robots. Experiments in Section 4 illustrate stability and demonstrate the advantages of our approach.

Notation: Vectors are bold lower case letters $\boldsymbol{a}$ and matrices bold capital letters $\boldsymbol{A}$. The Moore-Penrose pseudo inverse is written $\boldsymbol{A}^+$. Derivatives w.r.t. time are represented by dots above the quantity $\dot{x} := \frac{dx}{dt}$. The v-th time derivative of x is $x^{(v)} := \frac{d^v x}{dt^v}$. The set of continuous functions that are v times continuously differentiable is denoted by $\mathcal{C}^v$. A set $\mathcal{K}$ in the subscript $\boldsymbol{A}_\mathcal{K}$ indicates the reduction of the quantity to the rows of the indices contained in the set. The symbols $\mathbf{0}$ and $\boldsymbol{I}$ denote zero and identity matrices. Dimensions may be specified in subscripts $\boldsymbol{I}_m$ where a single dimension denotes a square matrix.

2. PRELIMINARIES

2.1 Robotic System

We consider a force controlled robotic system represented by the non-linear dynamics

$$\boldsymbol{M}(\boldsymbol{q})\ddot{\boldsymbol{q}} + \boldsymbol{C}(\boldsymbol{q},\dot{\boldsymbol{q}})\dot{\boldsymbol{q}} + \boldsymbol{g}(\boldsymbol{q}) = \boldsymbol{\tau}_\mathrm{c} \tag{1}$$

with generalized coordinates $\boldsymbol{q} \in \mathbb{R}^m$, and $\boldsymbol{\tau}_\mathrm{c} \in \mathbb{R}^m$ being the joint torques. The terms $\boldsymbol{M}(\boldsymbol{q}) \in \mathbb{R}^{m\times m}$, $\boldsymbol{C}(\boldsymbol{q},\dot{\boldsymbol{q}}) \in \mathbb{R}^{m\times m}$ and $\boldsymbol{g}(\boldsymbol{q}) \in \mathbb{R}^m$ denote the positive definite mass matrix, the Coriolis matrix, and the gravitational torques respectively. This system has the states $\boldsymbol{x}^T = [\boldsymbol{q}^T, \dot{\boldsymbol{q}}^T]^T$ with $\boldsymbol{x} \in \mathbb{R}^{2m=n}$ and is reformulated to

$$\dot{\boldsymbol{x}} = \begin{bmatrix}\dot{\boldsymbol{q}}\\ \ddot{\boldsymbol{q}}\end{bmatrix} = \underbrace{\begin{bmatrix}\dot{\boldsymbol{q}}\\ \boldsymbol{M}^{-1}(-\boldsymbol{g}-\boldsymbol{C}\dot{\boldsymbol{q}})\end{bmatrix}}_{\boldsymbol{f}(\boldsymbol{x})} + \underbrace{\begin{bmatrix}\mathbf{0}\\ \boldsymbol{M}^{-1}\end{bmatrix}}_{\boldsymbol{G}(\boldsymbol{x})}\boldsymbol{\tau}_\mathrm{c}\,. \tag{2}$$

In the following we omit time and non-linear dependencies of the parameters for notational simplicity. Without the supervising invariance control, the robot is directly controlled by a nominal control $\boldsymbol{\tau}_\mathrm{c} = \boldsymbol{\tau}_\mathrm{no}$ of impedance-type

$$\boldsymbol{\tau}_\mathrm{no} = -\boldsymbol{K}(\boldsymbol{q}-\boldsymbol{q}_d) - \boldsymbol{D}\dot{\boldsymbol{q}} + \boldsymbol{g}(\boldsymbol{q})\,, \tag{3}$$

where $\boldsymbol{K} \in \mathbb{R}^{m\times m}$ and $\boldsymbol{D} \in \mathbb{R}^{m\times m}$ are symmetric and positive definite stiffness and damping matrices. The desired configuration of the robot is denoted by $\boldsymbol{q}_d \in \mathbb{R}^m$.

2.2 Invariance Control and Augmentation

The idea of invariance control as presented in (Kimmel and Hirche, 2015) is the supervision of a nominal control w.r.t. a set of time varying hard constraints $h_i(\boldsymbol{x}(t),\boldsymbol{\eta}(t)) \in \mathbb{R}$, $i \in \{1,2...,l\}$ with relative degrees $r_i \in \mathbb{N}$ to switch between nominal and corrective control, whenever necessary to enforce the constraints. The functions $h_i(\boldsymbol{x}(t),\boldsymbol{\eta}(t))$ parametrized by $\boldsymbol{\eta}(t) \in \mathbb{R}^{n_\eta}$ define the set of constraints limiting the state space of the system to the admissible set

$$\mathcal{H}(t) = \{\boldsymbol{x} \in \mathbb{R}^n \,|\, h_i(\boldsymbol{x}(t),\boldsymbol{\eta}(t)) \le 0 \;\forall\, i \in \{1,2,...l\}\}\,. \tag{4}$$

The switching policy is based on so called invariance functions $\Phi_i(\boldsymbol{x}(t),\boldsymbol{\eta}(t),...,\boldsymbol{\eta}^{(r_i-1)}(t),\gamma_i) \in \mathbb{R}$ which are worst-case predictions for h_i given the current states $\boldsymbol{x}$ and assuming a maximum constant reaction of the robot in direction of the constraint $h_i^{(r_i)} = \gamma_i$. Here, the parameter γ_i is equivalent to a maximum relative acceleration. The derivation of Φ_i is based on an I/O-linearisation of h_i

$$z_i = h_i^{(r_i)} = \boldsymbol{a}_i^T(\boldsymbol{x},\boldsymbol{\eta}_i)\boldsymbol{\tau}_\mathrm{c} + b_i(\boldsymbol{x},\boldsymbol{\eta}_i,\dot{\boldsymbol{\eta}}_i,...,\boldsymbol{\eta}_i^{(r_i)})\,. \tag{5}$$

with vector $\boldsymbol{a}_i \in \mathbb{R}^m$ describing the influence of the control input $\boldsymbol{\tau}_\mathrm{c}$ on constraint i and $b_i \in \mathbb{R}$ containing all residual terms which includes e.g. motion of the constraint surfaces expressed by the time-varying parameters $\boldsymbol{\eta}(t)$. In case corrective control is applied, constraints in the vector space of $\boldsymbol{\tau}_\mathrm{c}$ as

$$h_i^{(r_i)} \overset{!}{\le} z_{\mathrm{c},i} \tag{6}$$

are set such that the system stays inside the admissible set (4). A simple choice to achieve this goal is $z_{\mathrm{c},i} = \gamma_i$ for an active constraint indicated by $\Phi_i \ge 0$. To reduce chattering in areas where $\Phi_i \simeq 0$ holds, more involved strategies are possible (Kimmel and Hirche, 2014). In order to achieve a minimum difference in terms of the Euclidean norm between corrective and nominal control, the system input $\boldsymbol{\tau}_\mathrm{c}$ is determined by solving the minimization problem

$$\begin{aligned}&\underset{\boldsymbol{\tau}_\mathrm{c}}{\operatorname{argmin}} ||\boldsymbol{\tau}_\mathrm{c} - \boldsymbol{\tau}_\mathrm{no}||_2\\ &\text{subject to } (6)\,.\end{aligned} \tag{7}$$

As long as no constraint is active, the solution of (7) is exactly $\boldsymbol{\tau}_\mathrm{no}$. For a set of linearly independent constraints $\mathcal{K}$ with $|\mathcal{K}| < m$ and a non-empty admissible set $\mathcal{H}$, problem (7) has an analytic solution given by

$$\boldsymbol{\tau}_\mathrm{c} = \boldsymbol{\tau}_\mathrm{no} + \boldsymbol{A}_\mathcal{K}^+(\boldsymbol{z}_{\mathcal{K},\mathrm{c}} - \boldsymbol{z}_{\mathcal{K},\mathrm{no}}) \tag{8}$$

according to (Kimmel and Hirche, 2015). The matrix $\boldsymbol{A}$ consists of the rows $\boldsymbol{a}_i^T$ from (5). An overall control structure of an invariance controlled robot is depicted in Figure 1. Between robot and nominal control, invariance control is set for supervision. Constraint tracking is required with dynamic boundaries to determine the parameters $\boldsymbol{\eta}(t)$ online.
This paper addresses the problem of jumps caused by invariance control in terms of system inputs $\boldsymbol{\tau}_\mathrm{c}$ by switching between nominal and corrective control. These discontinuities can be solved applying an augmented version of invariance control as proposed in (Kimmel et al., 2016).

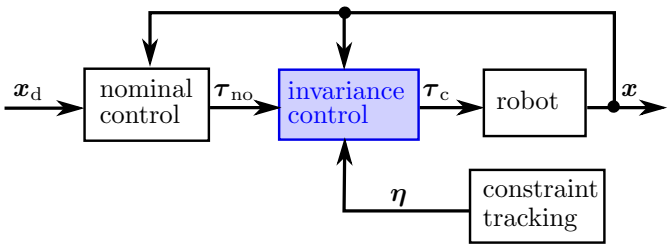

Fig. 1. Control scheme of a robot supervised by a non-augmented invariance control (blue).

The key idea is to move the corrective switching to a higher relative degree by artificially adding dynamics on the control input of the system, introducing additional states $\boldsymbol{\chi} \in \mathbb{R}^{m \cdot v}$ where $v \in \mathbb{N}$ denotes the degree of augmentation. The augmented dynamics of a generic control affine system is

$$\begin{bmatrix} \dot{\boldsymbol{x}} \\ \dot{\boldsymbol{\chi}} \end{bmatrix} = \begin{bmatrix} \boldsymbol{f}(\boldsymbol{x}) + \boldsymbol{G}(\boldsymbol{x})\boldsymbol{\tau}_\mathrm{c} \\ \boldsymbol{f}_\mathrm{a}(\boldsymbol{\chi}) \end{bmatrix} + \begin{bmatrix} \boldsymbol{0} \\ \boldsymbol{G}_\mathrm{a}(\boldsymbol{\chi}) \end{bmatrix} \boldsymbol{\tau}_\mathrm{ac}\,. \tag{9}$$

where the smooth vector field $\boldsymbol{f}_\mathrm{a} \in \mathbb{R}^{m \cdot v}$ and the matrix $\boldsymbol{G}_\mathrm{a} \in \mathbb{R}^{m \cdot v \times m}$ represent the added control affine dynamics. The augmented control input to system (9) is $\boldsymbol{\tau}_\mathrm{ac} \in \mathbb{R}^m$ which can be considered a higher relative degree version of the $\boldsymbol{\tau}_\mathrm{c}$. We use it to design the augmented invariance control scheme with higher relative degrees of the contraints $r_{\mathrm{a},i} = r_i + v$ and using (5)-(8). Corrective control actions to enforce the constraints are now performed using the higher order pseudo input chosen e.g. as a derivative of $\boldsymbol{\tau}_\mathrm{c}$. It is obvious that corrective and nominal control have to act on the system at the same relative degree to achieve smoother behaviour and for the principles of invariance control to be applicable. For $v > 0$, this is not the case with control (3). A solution to this problem is given in (Kimmel et al., 2016) by

$$\boldsymbol{\tau}_\mathrm{ano} = \boldsymbol{A}_\mathrm{a}^{-1}(\boldsymbol{\chi}) \left(\boldsymbol{\tau}_\mathrm{no}^{(v)} - \boldsymbol{b}_\mathrm{a}(\boldsymbol{\chi}) - \sum_{j=0}^{v-1} k_j (\boldsymbol{\tau}_\mathrm{c}^{(j)} - \boldsymbol{\tau}_\mathrm{no}^{(j)}) \right) \tag{10}$$

as augmented nominal control that may be interpreted as a filtered version of the original control with time constants defined through the gains $k_j > 0$. For non-active constraints, $\boldsymbol{\tau}_\mathrm{ac} = \boldsymbol{\tau}_\mathrm{ano}$ is applied as input to the augmented system. The matrix $\boldsymbol{A}_\mathrm{a} \in \mathbb{R}^{m \times m}$ and the vector $\boldsymbol{b}_\mathrm{a} \in \mathbb{R}^m$ result from the I/O-linearisation of $\boldsymbol{\tau}_\mathrm{c}$ w.r.t. $\boldsymbol{\tau}_\mathrm{ac}$

$$\boldsymbol{\tau}_\mathrm{c}^{(v)} = \boldsymbol{A}_\mathrm{a}(\boldsymbol{\chi})\boldsymbol{\tau}_\mathrm{ac} + \boldsymbol{b}_\mathrm{a}(\boldsymbol{\chi}) \tag{11}$$

where $\boldsymbol{A}_\mathrm{a}$ must be invertible which is the case if $\boldsymbol{\tau}_\mathrm{c}$ has a vector relative degree of $(v, v, ..., v)$ w.r.t. $\boldsymbol{\tau}_\mathrm{ac}$. This motivates the following assumption:

Assumption 1. The additional dynamics $\boldsymbol{f}_\mathrm{a}$, $\boldsymbol{G}_\mathrm{a}$ from (9) are chosen such that $\boldsymbol{\tau}_\mathrm{c}$ has a vector relative degree of $(v, v, ..., v)$ w.r.t. $\boldsymbol{\tau}_\mathrm{ac}$.

As an example, the choice $\boldsymbol{A}_\mathrm{a} = \boldsymbol{I}_m$, $\boldsymbol{b}_\mathrm{a} = \boldsymbol{0}$ fulfils Assumption 1 and implements the added dynamics as a simple integrator chain. Equation (10) achieves that for non-active constraints, the control input $\boldsymbol{\tau}_\mathrm{c}$ converges to $\boldsymbol{\tau}_\mathrm{no}$ according to (Kimmel et al., 2016) and under the assumption that $\boldsymbol{\tau}_\mathrm{no}$ is v times differentiable.

Assumption 2. The nominal control input $\boldsymbol{\tau}_\mathrm{no}$ is at least v times continuously differentiable w.r.t. time, i.e. $\boldsymbol{\tau}_\mathrm{no} \in \mathcal{C}^{v_+}$, $v_+ \in \mathbb{N}$, $v_+ \geq v$.

The depicted approach to augmented invariance control is applied in this paper to perform collision avoidance with an impedance controlled robot, achieving continuous control inputs. Therefore the following section serves to adapt the theory of augmented invariance control to a robot setting proving asymptotic stability based on Lyapunov theory.

3. AUGMENTED INVARIANCE CONTROL FOR IMPEDANCE-CONTROLLED ROBOTS

3.1 Nominal Control and Dynamics

The generic augmented dynamics (9) allow for any $\boldsymbol{f}_\mathrm{a}$, $\boldsymbol{G}_\mathrm{a}$ that fulfil assumption 1. For reasons of simplicity and interpretability we define the added dynamics to be pure integrator chains of higher order time derivatives of the control input $\boldsymbol{\tau}_\mathrm{c}$.

Assumption 3. The dynamics $\boldsymbol{f}_\mathrm{a}$, $\boldsymbol{G}_\mathrm{a}$ from (9) are chosen to be integrator chains, meaning $\boldsymbol{A}_\mathrm{a} = \boldsymbol{I}_m$ and $\boldsymbol{b}_\mathrm{a} = \boldsymbol{0}$.

With this assumption, (11) simplifies to $\boldsymbol{\tau}_\mathrm{c}^{(v)} = \boldsymbol{\tau}_\mathrm{ac}$ which we insert into (10), yielding the augmented nominal control

$$\boldsymbol{\tau}_\mathrm{ano} = \boldsymbol{\tau}_\mathrm{no}^{(v)} - \sum_{j=0}^{v-1} k_j (\boldsymbol{\tau}_\mathrm{c}^{(j)} - \boldsymbol{\tau}_\mathrm{no}^{(j)})\,. \tag{12}$$

Introducing the error $\boldsymbol{\Delta} \in \mathbb{R}^{m \cdot v}$

$$\boldsymbol{\Delta} = \begin{bmatrix} \boldsymbol{\Delta}_0 \\ \boldsymbol{\Delta}_1 \\ ... \\ \boldsymbol{\Delta}_{v-1} \end{bmatrix} = \begin{bmatrix} \boldsymbol{\tau}_\mathrm{no} - \boldsymbol{\tau}_\mathrm{c} \\ \dot{\boldsymbol{\tau}}_\mathrm{no} - \dot{\boldsymbol{\tau}}_\mathrm{c} \\ ... \\ \boldsymbol{\tau}_\mathrm{no}^{(v-1)} - \boldsymbol{\tau}_\mathrm{c}^{(v-1)} \end{bmatrix} \tag{13}$$

we reformulate the augmented dynamics (9) under augmented nominal control (12) with $\boldsymbol{\tau}_\mathrm{no}$ from (3) to

$$\begin{bmatrix} \dot{\boldsymbol{q}} \\ \ddot{\boldsymbol{q}} \\ \dot{\boldsymbol{\Delta}} \end{bmatrix} = \begin{bmatrix} \dot{\boldsymbol{q}} \\ \boldsymbol{M}^{-1}(-\boldsymbol{K}(\boldsymbol{q} - \boldsymbol{q}_d) - \boldsymbol{D}\dot{\boldsymbol{q}} - \boldsymbol{C}\dot{\boldsymbol{q}} - \boldsymbol{S}_0\boldsymbol{\Delta}) \\ [\boldsymbol{S}_{\bar{0}}^T,\ -\boldsymbol{K}_\mathrm{a}^T]^T\boldsymbol{\Delta} \end{bmatrix}. \tag{14}$$

The gain matrix $\boldsymbol{K}_\mathrm{a} \in \mathbb{R}^{m \times m \cdot v}$ can be written as $\boldsymbol{K}_\mathrm{a} = [k_0\boldsymbol{I}_m,\, k_1\boldsymbol{I}_m,\, ...,\, k_{v-1}\boldsymbol{I}_m]$ and the selection matrices $\boldsymbol{S}_0 \in \mathbb{R}^{m \times m \cdot v}$ and $\boldsymbol{S}_{\bar{0}} \in \mathbb{R}^{m \cdot (v-1) \times m \cdot v}$ are defined by $\boldsymbol{S}_0 = [\boldsymbol{I}_m,\, \boldsymbol{0}_{m \times m \cdot (v-1)}]$ and $\boldsymbol{S}_{\bar{0}} = [\boldsymbol{0}_{m \cdot (v-1) \times m},\, \boldsymbol{I}_{m \cdot (v-1)}]$ respectively. As only $\boldsymbol{\Delta}_0 = \boldsymbol{\tau}_\mathrm{no} - \boldsymbol{\tau}_\mathrm{c}$ directly influences the joint accelerations $\ddot{\boldsymbol{q}}$, we select it with $\boldsymbol{S}_0\boldsymbol{\Delta} = \boldsymbol{\Delta}_0$. All remaining elements in $\boldsymbol{\Delta}$ besides $\boldsymbol{\Delta}_0$ are selected by $\boldsymbol{S}_{\bar{0}}$.

3.2 Stability

The proof of stability from (Kimmel et al., 2016) for augmented nominal control is formulated for exponentially stabilizing nominal controls. To our best knowledge, exponential stability could not be proven for impedance-controlled robots, motivating the following theorem.

Theorem 1. Let Assumptions 1-3 hold. Then the system (1) under control (12) with $\boldsymbol{\tau}_\mathrm{no}$ from (3) is uniformly asymptotically stable in the sense of Lyapunov.

Proof:
We assume that the desired joint configuration is in the origin $\boldsymbol{q}_d = \boldsymbol{0}$. This is no mayor restriction as for $\boldsymbol{q}_\mathrm{d} \neq \boldsymbol{0}$ we can always transform (2) to meet this assumption. The Lyapunov function

$$V(\boldsymbol{q}, \dot{\boldsymbol{q}}, \boldsymbol{\Delta}) = \frac{1}{2}\boldsymbol{q}^T\boldsymbol{K}\boldsymbol{q} + \frac{1}{2}\dot{\boldsymbol{q}}^T\boldsymbol{M}\dot{\boldsymbol{q}} + \frac{1}{2}\boldsymbol{\Delta}^T\boldsymbol{P}\boldsymbol{\Delta} \tag{15}$$

contains the virtual energy stored in the virtual spring of the impedance control $\boldsymbol{q}^T\boldsymbol{K}\boldsymbol{q}$, the kinetic energy of the system $\dot{\boldsymbol{q}}^T\boldsymbol{M}\dot{\boldsymbol{q}}$, and the pseudo energy term $\boldsymbol{\Delta}^T\boldsymbol{P}\boldsymbol{\Delta}$ that serves as a positive definite storage function for the states added due to augmentation. The matrix $\boldsymbol{P} \in \mathbb{R}^{m \cdot v \times m \cdot v}$ is symmetric and positive definite. Also $V(\boldsymbol{0}, \boldsymbol{0}, \boldsymbol{0}) = 0$ holds,

making V a suitable Lyapunov candidate. Differentiation of (15) gives

$$\begin{aligned}\dot{V} = \dot{\boldsymbol{q}}^T \boldsymbol{K}\boldsymbol{q} + \dot{\boldsymbol{q}}^T(-\boldsymbol{K}\boldsymbol{q} - \boldsymbol{D}\dot{\boldsymbol{q}} - \boldsymbol{C}\dot{\boldsymbol{q}} - \boldsymbol{S}_0\boldsymbol{\Delta}) \\ + \frac{1}{2}\dot{\boldsymbol{q}}^T\dot{\boldsymbol{M}}\dot{\boldsymbol{q}} + \boldsymbol{\Delta}^T\left[\boldsymbol{S}_0^T,\, -\boldsymbol{K}_\mathrm{a}^T\right]^T\boldsymbol{P}\boldsymbol{\Delta}\end{aligned} \tag{16}$$

where we insert the skew-symmetry property of mass and Coriolis matrices $\dot{\boldsymbol{q}}^T(\dot{\boldsymbol{M}} - 2\boldsymbol{C})\dot{\boldsymbol{q}} = \boldsymbol{0}$, (Murray et al., 1994) and simplify to

$$\dot{V} = -\dot{\boldsymbol{q}}^T\boldsymbol{D}\dot{\boldsymbol{q}} + \boldsymbol{\Delta}^T\left[\boldsymbol{S}_0^T,\, -\boldsymbol{K}_\mathrm{a}^T\right]^T\boldsymbol{P}\boldsymbol{\Delta} - \dot{\boldsymbol{q}}^T\boldsymbol{S}_0\boldsymbol{\Delta} \tag{17}$$

which is zero at the origin $\boldsymbol{x} = \boldsymbol{0}$, $\boldsymbol{\Delta} = \boldsymbol{0}$. A symmetric positive definite matrix $\boldsymbol{P}$ always exists that satisfies the inequality

$$\dot{V}(\dot{\boldsymbol{q}}, \boldsymbol{\Delta}) \leq 0 \tag{18}$$

and thus renders $\dot{V}(\dot{\boldsymbol{q}}, \boldsymbol{\Delta})$ negative semi-definite, considering that the states $\boldsymbol{q}$ are not contained in $\dot{\boldsymbol{V}}$. To illustrate this claim, consider the exemplary choice for $\boldsymbol{P}$

$$\boldsymbol{P} = \begin{bmatrix} p_1\boldsymbol{I}_{m\cdot(v-1)} & \boldsymbol{0} \\ \boldsymbol{0} & p_2\boldsymbol{I}_m \end{bmatrix} \tag{19}$$

with positive scalar parameters $p_1 > 0$ and $p_2 > 0$. Let $p_1 << p_2$ and $p_1 << 1$ hold. We rearrange the terms in (17) into negative definite and indefinite terms by splitting the quadratic form of $\boldsymbol{\Delta}$.

$$\begin{aligned}\dot{V} = &\underbrace{-\dot{\boldsymbol{q}}^T\boldsymbol{D}\dot{\boldsymbol{q}} - \boldsymbol{\Delta}^T\left[\boldsymbol{0},\, p_2\boldsymbol{K}_\mathrm{a}^T\boldsymbol{I}_m\right]^T\boldsymbol{\Delta}}_{\text{negative definite}} \\ &\underbrace{-\dot{\boldsymbol{q}}^T\boldsymbol{S}_0\boldsymbol{\Delta} + \boldsymbol{\Delta}^T\left[p_1\boldsymbol{S}_0^T\boldsymbol{I}_{m(v-1)},\, \boldsymbol{0}\right]^T\boldsymbol{\Delta}}_{\text{finite, indefinite}}\end{aligned} \tag{20}$$

It is obvious that the term $\boldsymbol{\Delta}^T[p_1\boldsymbol{S}_0^T\boldsymbol{I}_{m(v-1)},\, \boldsymbol{0}]^T\boldsymbol{\Delta}$ tends to 0 for $p_1 \to 0$ and that for large enough values p_2 and finite states $\boldsymbol{\Delta}$ and $\dot{\boldsymbol{q}}$, we render $\dot{V}$ negative semi-definite. At this point we have proven semi-global uniform stability of the system according to Theorem 4.1 of (Khalil, 1996). Applying LaSalle's invariance principle proves asymptotic stability, which is omitted at this point for the sake of brevity. □

Given that the invariance control scheme ensures that the system stays inside the admissible set, we argue that the system will always eventually come back to a state without active constraints, where the augmented nominal control asymptotically stabilizes the system. In case of active constraints, the corrections will only influence $\boldsymbol{\tau}_\mathrm{ac}$ in direction of the constraints. Perpendicular to the constraints, still nominal control is applied. A phenomenon that might occur due to the I/O-linearisation of the constrains h_i are internal dynamics. It is shown in (Kimmel et al., 2016) that under Assumption 1, no additional internal dynamics arise due to the performed augmentation. This motivates introducing the following assumption:

Assumption 4. The I/O-linearisation of $h_i\, \forall\, i \in \{1, 2, .., l\}$ given system (2) yields stable internal dynamics.

3.3 Exemplary Control Design

For the experiments of this work, an invariance control is implemented that achieves continuous actuation in an obstacle avoidance scenario. A non-augmented invariance control in combination with a torque controlled robot switches between nominal and corrective control on the level of torques, resulting in discontinuous control inputs $\boldsymbol{\tau}_\mathrm{c}$ and state trajectories that are $\boldsymbol{x}(t) \in \mathcal{C}^0$ which describes a vectorial function that is continuous but not continuously differentiable. Our goal is to achieve

$$\boldsymbol{\tau}_\mathrm{c}(t) \overset{!}{\in} \mathcal{C}^0\ ,\ \boldsymbol{x}(t) \overset{!}{\in} \mathcal{C}^1\,. \tag{21}$$

Thus, we need to augment the system by $v = 1$. Inserting into (9) and with Assumption 3 we obtain

$$\dot{\boldsymbol{x}}_\mathrm{a} = \begin{bmatrix} \dot{\boldsymbol{x}} \\ \dot{\boldsymbol{\tau}}_\mathrm{c} \end{bmatrix} = \begin{bmatrix} \boldsymbol{f}(\boldsymbol{x}) + \boldsymbol{G}(\boldsymbol{x})\boldsymbol{\tau}_\mathrm{c} \\ \boldsymbol{\tau}_\mathrm{ac} \end{bmatrix} \tag{22}$$

as augmented dynamics with $\boldsymbol{x}_\mathrm{a} \in \mathbb{R}^{n+m}$ denoting the states of the augmented system. In collision avoidance scenarios as considered in this paper, constraints are set on position level and thus have a relative degree of $r_i = 2$. For $v = 1$ this means that $r_{\mathrm{a},i} = 3$ holds. From (Wolff and Buss, 2004) we know that we obtain an upper bound for future values of a constraint h_i of relative degree 3 assuming a constant $h_i^{(3)} = \gamma_i$ by

$$h_i(t + t_f) \leq \underbrace{\frac{t_f^3}{6}\gamma_i + h_i(t) + t_f\dot{h}_i(t) + \frac{1}{2}t_f^2\ddot{h}_i(t)}_{p_i(t, t_f, \gamma_i)} \tag{23}$$

with $t_f \in \mathbb{R}, t_f > t$ being a time in the future and the upper bound polynomial $p_i(t, t_f, \gamma_i)$. The predicted maximum value of h_i, given the relative degree of 3, is reached at t_max

$$t_\mathrm{max} = -\frac{\ddot{h}_i}{\gamma_i} + \sqrt{\frac{\ddot{h}_i^2}{\gamma_i^2} - 2\frac{\dot{h}_i}{\gamma_i}}\,. \tag{24}$$

Defining that the maximum reaction of the robot to the constraint $h_i^{(r_{\mathrm{a},i})} = \gamma_i$ we thus obtain a precise worst case prediction and define the invariance function by

$$\Phi_i = \begin{cases} h(t) & ,\ (\mathrm{I}) \vee (\mathrm{II}) \\ p_i(t, t_\mathrm{max}, \gamma_i) & ,\ \text{else} \end{cases} \tag{25}$$

with the sets
(I) $= \{\boldsymbol{x}, \boldsymbol{\eta}(t)\,|\,\dot{h}_i \leq 0 \wedge \ddot{h}_i \leq 0\}$
(II) $= \{\boldsymbol{x}, \boldsymbol{\eta}(t)\,|\,\ddot{h}_i^2 - 2\dot{h}_i\gamma_i < 0\}$.
This gives us all we need to determine whether constraints are active and when to use (5)-(7) to calculate the corrective control. Therefore, a valid choice of $z_{\mathrm{c},i}$ is necessary. To stay inside the admissible set, one needs to assure that the invariance functions of active constraints are locally decreasing at the boundaries $\partial\Phi$ of the set $\{\Phi_i \leq 0, \forall i \in \{1, 2, .., l\}\}$ which is thereby rendered positively invariant. Once the system entered, it will always stay inside this invariant set. Two further goals that influence our choice of $z_{\mathrm{c},i}$ is that we want to apply nominal control whenever possible, and that unnecessary chattering at the boundaries should be avoided. We therefore propose to deviate from the simple choice of setting $z_{\mathrm{c},i} = \gamma_i$, $\forall i \in \{i|\Phi_i \geq 0\}$ and to apply

$$z_{\mathrm{c},i} = \begin{cases} z_{\mathrm{no},i} & ,\ (\mathrm{III}) \\ \min(z_{\mathrm{no},i}, \gamma_i) & ,\ (\mathrm{IV}) \\ \min(z_{\mathrm{no},i}, 0) & ,\ \text{else} \end{cases} \tag{26}$$

with the sets (III) and (IV) defined as:
(III) $= \{\boldsymbol{x}, \boldsymbol{\eta}, \dot{\boldsymbol{\eta}}, \ddot{\boldsymbol{\eta}}|\ \Phi_i < 0\ \}$
(IV) $= \{\boldsymbol{x}, \boldsymbol{\eta}, \dot{\boldsymbol{\eta}}, \ddot{\boldsymbol{\eta}}|\ [\Phi_i \geq 0 \wedge (\dot{h}_i > 0 \vee \ddot{h}_i > 0)] \vee$
$(\Phi_i > 0 \wedge \dot{h}_i = 0 \wedge \ddot{h}_i = 0)\}$. Finally we insert $v = 1$ and $\dot{\boldsymbol{\tau}}_\mathrm{c} = \boldsymbol{\tau}_\mathrm{ac}$ into (12) yielding

$$\boldsymbol{\tau}_\mathrm{ano} = \dot{\boldsymbol{\tau}}_\mathrm{no} - k_0(\boldsymbol{\tau}_\mathrm{c} - \boldsymbol{\tau}_\mathrm{no}) \tag{27}$$

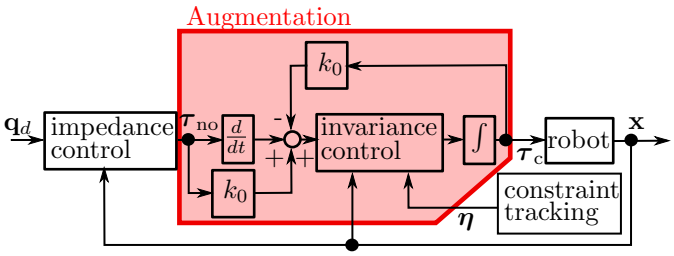

Fig. 2. Closed loop system with a ($v = 1$)-augmented invariance control scheme. The red area marks the augmented invariance control implemented for the experiments of this paper.

as the augmented nominal control. The resulting closed loop system is illustrated in Figure 2. The area indicated in red marks the augmented invariance control. Compared to the original scheme in Figure 1, nominal control is differentiated prior to supervision. Integration of the corrected signal yields the input to the robotic system.

Remark: Unlike e.g. potential field methods, augmented invariance control *guarantees* constraint adherence under significant dynamics. Additionally, it can be combined with a broad variety of nominal controls allows high flexibility and modularity in the control design in contrast to e.g. MPC. The optimal invariance control can be found analytically despite non-linear dynamics and boundaries making the approach computationally efficient and therefore highly applicable when real-time matters as in robot force control schemes.

4. EXPERIMENTAL EVALUATION

4.1 Setup and Procedure

To compare the approach of augmented invariance control from Section 3 with a non-augmented version, both approaches were implemented based on the robot operating system ROS to perform obstacle avoidance in task space with a KUKA-LWR4+. Therefore the end-effector of the KUKA arm is here geometrically modelled as a sphere, centred at the last link of the arm. A spherical obstacle is simulated to pass the end-effector, forcing the arm to deviate in order to keep the hard constraint formulated on the Euclidean distance of the surfaces of end-effector and obstacle geometry. This scenario is illustrated in Figure 3. The simulation of the obstacle allows for identical conditions for both approaches such that the results yield a valid comparison of performance. Parameters appearing in both approaches where therefore chosen equally as listed in Table 1. A Cartesian formulation of impedance control is applied as nominal control in the shape of

$$\boldsymbol{\tau}_c = \boldsymbol{J}^T(\boldsymbol{q})(-K_C(\boldsymbol{p} - \boldsymbol{p}_d) - D_C\dot{\boldsymbol{p}}) + \boldsymbol{g}(\boldsymbol{q}) \qquad (28)$$

where $K_C \in \mathbb{R}$ and $D_C \in \mathbb{R}$ are positive stiffness and damping gains and the Jacobian $\boldsymbol{J}(\boldsymbol{q})$ serves to map from Cartesian task space to joint space. The test scenario and the resulting avoidance motion of the robot are depicted in Figure 3. The spherical obstacle passes with a velocity $v_{\text{obs}} = 0.1\text{m/s}$ by the end-effector link from left to right. A mainly vertical deviation of the robot is caused by the constrained Euclidean distance. After the obstacle passed, nominal control brings the arm back to the desired position. Relevant data is published as topics using the publish/subscribe framework of ROS. The experimental

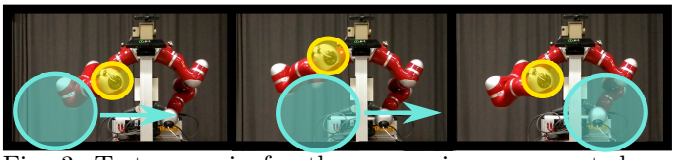

Fig. 3. Test scenario for the comparison augmented vs. non-augmented invariance control for obstacle avoidance. Hard constraints are defined on the Euclidean distance between end-effector link (yellow) and the dynamic obstacle (cyan).

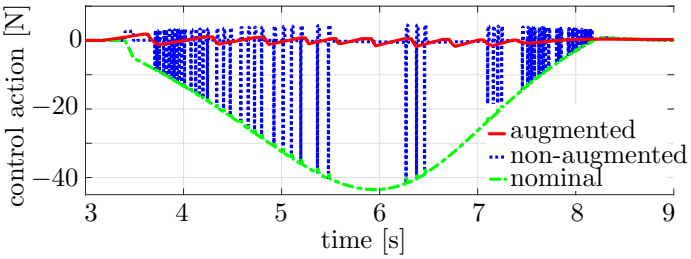

Fig. 4. Vertical forces applied during obstacle avoidance with augmented (red) and non-augmented invariance control (blue). The augmented version shows a smooth behaviour with lower absolute forces and less chattering. The depicted forces do not contain gravity.

data was recorded in ROS-bags and is analysed in the following section.

4.2 Results

The experiments successfully demonstrated the stability of the approach as well as the benefits of augmenting invariance control. A major difference is observed w.r.t. the actuation $\boldsymbol{\tau}_c$ which is illustrated in Figure 4. It shows vertical forces, as this is the main direction of both corrective control and motion in the experiments. The non-augmented version executes jumps between nominal and corrective control due to chattering, while the augmented control achieves the desired smooth behaviour in terms of a continuous actuation. Besides avoiding jumps, the augmented implementation manages to perform the obstacle avoidance with far lower absolute forces. On average, the integrated absolute actuation during the experiments was reduced by about 89.7% in average with the augmented approach. The maximum forces are even reduced by about 40.1N which represents a reduction of circa 92.6% compared to the non-augmented approach. These results indicate a drastically reduced load for the robot

Table 1. Key parameters for the experiment comparing augmented and non-augmented invariance control in an obstacle avoidance scenario.

parameter	**non-augmented**	**augmented**
K_C	300.0N/m	300.0N/m
D_C	100.0Ns/m	100.0Ns/m
r_{eff}	0.1m	0.1m
r_{obs}	0.2m	0.2m
γ	−1.0	−1.0
k_0	–	1.0s^{-1}
v_{obs}	0.1m/s	0.1m/s
$f_{\text{control,Hz}}$	500Hz	500Hz

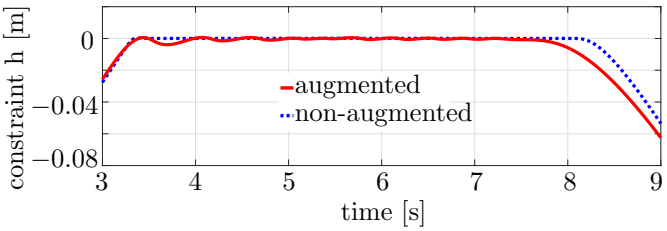

Fig. 5. Constraint h during obstacle avoidance. Both approaches achieve adherence to the constraint $h \leq 0$.

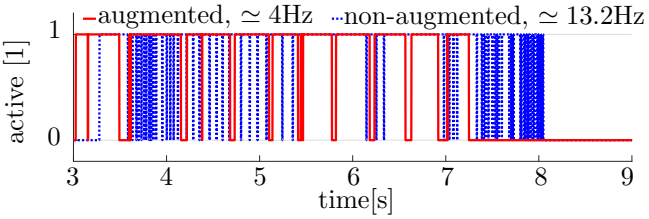

Fig. 6. Chattering during obstacle avoidance. The average chattering frequency is reduced by about 70% with augmented invariance control.

actuation with the proposed control. Also both approaches manage to keep the constraint h which is plotted in Figure 5. While the augmented approach shows minor initial oscillation at the boundary $h = 0$, the non-augmented control sticks close to the boundary from the beginning of the avoiding motion at about 3.5s. This oscillation comes from the type of augmentation integral filter and can be reduced by adjusting filter parameters. This is beyond the scope of this paper and may be regarded as higher relative degree chattering as is observable in Figure 6, which shows when the constraint is active using Boolean variables (0 for non-active, 1 for active). At the boundaries the augmented approach outperforms the non-augmented version. Some chattering occurs for both approaches due to the discrete time implementation. Both control schemes are evaluated at a frequency of 500Hz, still the exact time when $\Phi = 0$ is reached is slightly missed causing chattering at the boundaries of the admissible set. These violations due to chattering need to be separately addressed (Kimmel and Hirche, 2014) and are not in the scope of this paper. A considerable difference between augmented and non-augmented approach is obvious regarding the average frequencies of chattering when the system slides along the $h = 0$ boundary ($\simeq$ 3.95Hz for augmented, $\simeq$ 13.20 Hz for non-augmented). In the conducted experiments the chattering frequency was reduced by about 70% in average by the augmentation showing another benefit of the proposed approach. The boundary violations due to chattering are at a sub-millimetre level and are considered negligible. Figure 6 shows that the augmented version reacts sooner to the approaching obstacle as the constraint is active by about 0.2s earlier. This is a result of the higher relative degree of corrective control and can be influenced in terms of the parameter γ. The experiments also showed that the augmented approach takes longer to return to the desired position after the obstacle avoidance motion. This is because the augmented version does not instantaneously jump back to nominal control but smoothly tracks it according to (27), causing a less direct tracking behaviour. This can be improved by introducing more complex dynamics $\boldsymbol{f}_a$ and $\boldsymbol{G}_a$, but is beyond the scope of this work.

5. CONCLUSION

This paper addresses the problem of augmented invariance control for impedance controlled robots. We show that stability characteristics are maintained when augmenting an impedance-type nominal control for invariance control. These results are validated in a collision avoidance experiment. The comparison to non-augmented invariance control shows promising results, especially regarding smoothness and control action. Lower control inputs to the system could be achieved by means of augmentation. As a positive side effect the influence of chattering was reduced. In turn, the workspace of the robot may be slightly reduced, as corrective actions at higher relative degrees may require earlier corrective reaction for preventing boundary violations. Future work will address the performance oriented design of the control scheme.

ACKNOWLEDGEMENTS

This work was supported by the EU Horizon2020 project RAMCIP, under grant agreement no. 643433.

REFERENCES

Angeli, D. and Mosca, E. (1999). Command governors for constrained nonlinear systems. *IEEE Transactions on Automatic Control*, 44(4), 816–820. doi: 10.1109/9.754825.

Khalil, H.K. (1996). *Nonlinear systems*. Prentice Hall, Upper Saddle River, (N.J.).

Kimmel, M., Jähne, C., and Hirche, S. (2016). Augmented invariance control for systems with smoothness constraints. In *Proceedings of the 55th Conference on Decision and Control (CDC)*. Las Vegas, USA.

Kimmel, M. and Hirche, S. (2014). Invariance Control with Chattering Reduction. *IEEE Conference on Decision and Control*, 68–74. doi:10.1109/CDC.2014.7039361.

Kimmel, M. and Hirche, S. (2015). Active Safety Control for Dynamic Human-Robot Interaction. 4685–4691. doi: 10.1109/IROS.2015.7354044.

Mayne, D.Q., Rawlings, J.B., Rao, C.V., and Scokaert, P.O. (2000). Constrained model predictive control: Stability and optimality. *Automatica*, 36(6), 789–814. doi:10.1016/S0005-1098(99)00214-9.

Murray, R.M., Sastry, S.S., and Zexiang, L. (1994). *A Mathematical Introduction to Robotic Manipulation*. CRC Press, Inc., Boca Raton, FL, USA, 1st edition.

Rauscher, M., Kimmel, M., and Hirche, S. (2016). Constrained robot control using control barrier functions. In *Proceedings of the IEEE/RSJ International Conference on Intelligent Robots and Systems (IROS)*, 7. Daejeon, Korea.

Rimon, E. and Koditschek, D. (1992). Exact Robot Navigation Using Artificial Potential Functions. *Robotics and Automation, IEEE*, 8(5), 501–518. doi: 10.1109/70.163777.

Wolff, J. and Buss, M. (2004). Invariance control design for nonlinear control affine systems under hard state constraints. *Proceedings of the NOLCOS 2004*, (2), 711–716.